Journal of Nuclear Medicine, published on June 21, 2017 as doi:10.2967/jnumed.117.194555

Pharmacokinetics, biodistribution, and radiation dosimetry for ^{89}Zr-trastuzumab in patients with esophagogastric cancer

Joseph A. O'Donoghue[1], Jason S. Lewis[2,3,4,5], Neeta Pandit-Taskar[3,4,6], Stephen E. Fleming[3,4], Heiko Schöder[3,4], Steven M. Larson[3,4,5,6], Volkan Beylergil[3], Shutian Ruan[3], Serge K. Lyashchenko[2,3], Pat B. Zanzonico[1], Wolfgang A. Weber[3,4,5], Jorge A. Carrasquillo[3,4,5,6]*, and Yelena Y. Janjigian[7,8]*

[1]Department of Medical Physics, Memorial Sloan Kettering Cancer Center (MSK), New York, NY; [2]Radiochemistry and Molecular Imaging Probes Core, MSK; [3]Department of Radiology, MSK; [4]Department of Radiology, Weill Cornell Medical Center (WCMD), New York, NY; [5]Molecular Pharmacology Program, MSK; [6]Center for Targeted Radioimmunotherapy and Diagnosis, Ludwig Center for Cancer Immunotherapy, New York, NY; [7]Department of Medicine, MSK; [8]Department of Medicine, WCMD, New York, NY. *contributed equally.

Corresponding Author: Jorge A. Carrasquillo, MD

1275 York Avenue

New York, NY 10065

Telephone: 212-639-2459

Fax: 212-717-3263

E-mail: carrasj1@mskcc.org

First Author: Joseph A. O'Donoghue, PhD

1275 York Avenue

New York, NY 10065

Telephone: 212-639-7417

E-mail: odonoghj@mskcc.org

Keywords: HER2, trastuzumab, ^{89}Zr, esophageal cancer, gastric cancer

Running title: ^{89}Zr-trastuzumab in EG cancer

Word count: 240 (abstract), 4,998 (full text)

Financial Support: Mr. William H. Goodwin and Mrs. Alice Goodwin and the Commonwealth Foundation for Cancer Research, The Center for Experimental Therapeutics of MSK, the Radiochemistry & Molecular Imaging Probes Core (NIH/NCI Cancer Center Support Grant P30 CA008748), the Ludwig Center for Cancer Immunotherapy at MSK, the Conquer Cancer Foundation (Career Development Award, to YYJ), the Department of Defense Congressionally Directed Medical Research Program (CA 150646, to YYJ, JSL, WAW), and the Geoffrey Beene Cancer Research Center at MSK (JSL). YYJ has received funding, or has pending grants or patents, from Boehringer Ingelheim, Bayer, Genentech, Bristol-Myers Squibb, Eli Lilly, Pfizer, and Merck.

ABSTRACT

Trastuzumab with chemotherapy improves clinical outcomes in patients with human epidermal growth factor receptor 2 (HER2)-positive esophagogastric adenocarcinoma (EGA). Despite the therapeutic benefit, responses are rarely complete and the majority of patients develop progression. This is the first report evaluating ^{89}Zr-trastuzumab in HER2-positive EGA in which we evaluate the safety, pharmacokinetics, biodistribution, and dosimetry. **Methods:** Trastuzumab was conjugated with deferoxamine and radiolabeled with ^{89}Zr. A mean activity of 184 MBq was administered to 10 patients with metastatic HER2-positive EGA. PET imaging, whole-body probe counts, and blood draws were performed to assess pharmacokinetics, biodistribution and dosimetry. **Results:** No clinically significant toxicities were observed. At the end of infusion, the estimated ^{89}Zr-trastuzumab in plasma volume was a median 102% (range 78-113%) of the injected dose. The median biologic $T_{1/2}$ β was 111 h (range 78-193 h). Median biologic whole-body retention half-life was 370 h (range 257-578 h). PET images showed optimal tumor visualization at 5-8 days post-injection. The maximum tumor standard uptake value (SUV) ranged from no to minimal uptake in three patients to a median of 6.8 (range 2.9-22.7) for 20 lesions in seven patients. Dosimetry estimates from Organ Level Internal Dose Assessment (OLINDA) showed that the organs receiving the highest absorbed doses were liver and heart wall with median values of 1.37 and 1.12 mGy/MBq, respectively. **Conclusion:** ^{89}Zr-trastuzumab imaging tracer is safe and provides high-quality

images in patients with HER2-positive EGA, with an optimal imaging time of 5-8 days post-injection.

INTRODUCTION

Gastric cancer is the fifth most common malignancy and among the leading causes of cancer death in the world (*1*). HER2 is a transmembrane receptor that is overexpressed in approximately 20% of EGAs (*2*). Trastuzumab, an anti-HER2 monoclonal antibody, is the first Food and Drug Administration-approved targeted agent to treat patients with EGA that overexpresses HER2 (*3*). However, not all patients with HER2-positive EGA respond to trastuzumab (*4*). Furthermore, duration of response to trastuzumab-containing therapy is only 6.7 months and the basis of resistance in EGA is an area of investigation.

In patients with HER2 expression in tumor, the heterogeneity of HER2 expression within primary tumors and metastases, as well as loss of HER2 expression while on trastuzumab therapy, are some factors that have been shown to contribute to therapeutic resistance (*5*). Furthermore, the extent of disease burden and presence of the primary tumor in the stomach has been shown to affect absorption, pharmacokinetics, and efficacy of trastuzumab and lapatinib (oral anti-HER2 tyrosine kinase inhibitor). An imaging agent that can non-invasively assess HER2 status and reflect functional effects of HER2-targeted agents in the primary tumor and metastases would help to elucidate these factors. Using ^{89}Zr-trastuzumab in gastric cancer xenografts, we demonstrated that ^{89}Zr-trastuzumab PET could delineate HER2-positive tumors and measure the pharmacodynamic effects of anti-HER2 therapy (*6*).

Previous reports with ^{89}Zr-trastuzumab have focused on its ability to detect breast cancer (*7*), determine HER2 tumor heterogeneity (*8*), and identify

patients likely to respond to HER2-directed treatments (*9,10*). Limited information is available on the pharmacokinetics and dosimetry of ^{89}Zr-labeled antibodies in general (*9-17*) and no detailed data on the pharmacokinetics of ^{89}Zr-trastuzumab has been published in peer-reviewed literature. Only recently has there been a report of ^{89}Zr-trastuzumab dosimetry in breast cancer (*18*). This is the first report evaluating ^{89}Zr-trastuzumab in HER2-positive EGA in which we evaluate the safety, pharmacokinetics, biodistribution, and dosimetry.

MATERIALS AND METHODS

Patients

Eligible patients had a diagnosis of HER2-positive metastatic EGA. Other eligibility criteria included measurable or evaluable disease by Response Evaluation Criteria in Solid Tumors version 1.1, Karnofsky performance $\geq$60%, and adequate organ function. Exclusion criteria included ejection fraction of <50% and known hypersensitivity to trastuzumab. For patients receiving trastuzumab, a washout period of at least 14 days was recommended.

Study Design and Cohorts

This was a single-site, prospective open-label imaging protocol. The study was approved by the institutional review board and ethics committees at Memorial Sloan Kettering Cancer Center (MSK) (ClinicalTrials.gov identifier

NCT02023996). All patients provided written informed consent. We report the results from the completed Cohort 1, of 10 patients who underwent serial ^{89}Zr-trastuzumab PET imaging (Supp. Fig. 1) to determine safety, biodistribution, pharmacokinetics, and dosimetry.

^{89}Zr-trastuzumab Drug Product

The ^{89}Zr-trastuzumab was manufactured by the MSK Radiochemistry and Molecular Imaging Probes Core Facility in compliance with an Food and Drug Administration investigational new drug application. Clinical-grade trastuzumab (Herceptin TM, Genentech, South San Francisco, CA) was conjugated with p-SCN-Bn-Deferoxamine (Macrocylics, Plano, TX) chelator, followed by radiolabeling with ^{89}Zr, a positron emitter with a 78.4 h half-life. The conjugation was performed using methodology previously described (*19*). The chelates:trastuzumab ratio was 1.03, as determined by the radioisotopic dilution method, with antibody concentration of 10.6 mg/mL, determined by ultraviolet-visible spectroscopy, and antibody monomer content of 100%, determined by SEC-HPLC. ^{89}Zr-oxalate was also prepared in-house as previously described (*20*) and used to radiolabel DFO-trastuzumab as previously described (*19,20*). The ^{89}Zr-trastuzumab final product had a radiochemical purity of more than 95%, endotoxin content of <5 EU/mL, pH of 5.5-8.0, and was sterile. Median immunoreactivity was 94% (range 86-97%) (*21*).

Patient unit doses of approximately 185 MBq/3 mg of ^{89}Zr-trastuzumab were mixed with non-radiolabeled trastuzumab to achieve a total mass of 50 mg.

The total antibody mass of 50 mg was selected based on literature experience (*7*). A mean of 184 MBq (range 182-189 MBq) was injected intravenously over ~5 min. Patients were monitored for two hours post-injection and any adverse effects were graded using Common Terminology Criteria for Adverse Events v. 4.

Imaging

All patients had dedicated computed tomography (CT) imaging as a reference standard a median of 9 days prior to (range 29 days prior to or 3 days after) ^{89}Zr-trastuzumab injection. Each patient underwent serial whole-body PET-CT scans from mid-skull to proximal thigh. All scans were performed on a GE Discovery STE PET/CT scanner (General Electric, Waukesha, WI) in 3D mode with attenuation, scatter, and other standard corrections applied and using iterative reconstruction. Images were acquired within 4 h of injection and at 1 day, 2-4 days, and 5-8 days post-injection using 3, 4, 5, and 7-8 min per bed position, respectively. Low-dose CT scans were used for attenuation correction using an X-ray tube current of 10 to 80 mA.

Images were read by an experienced nuclear medicine physician who was aware of the patient's history and conventional imaging (JAC). Localization in tumor was defined as focal accumulation greater than adjacent background in areas where physiologic activity was not expected. Volumes of interest were drawn on PET-CT images over normal liver, kidney, spleen, bone marrow, and lung using a dedicated workstation (Hermes Medical Solution Stockholm, Sweden and/or GE AW server 2.0) and over selected tumor lesions confirmed on

CT or FDG-PET. Standardized uptake values normalized to lean body mass (SUV_{LBM}) were determined.

Whole-body and Serum Clearance Measurements

Whole-body clearance was determined by serial measurements of count-rate using a 12.7 cm-thick NaI(Tl) scintillation detector at a fixed 3 m from the patient. Background-corrected geometric mean counts were obtained after infusion and before first voiding, immediately after first voiding, and subsequently at the times of the PET scans. Count rates were normalized to the immediate post-infusion value (taken as 100%) to yield relative retained activities (in %).

Blood samples were obtained at approximately 5, 15, 30, 60 min, and 2 h after injection, and on subsequent days of each PET scan (n=8). Aliquots of serum were counted using a well-type detector (Wallac Wizard 1480 gamma counter, Perkin Elmer). The measured activity concentrations were converted to percent injected activity/liter (% IA/L).

The whole-body probe data and the serum activity concentration data was fit using monoexponential or bi-exponential function using SAAM software (*22*). This data was used to determine cumulated activity per unit administered activity (i.e., residence time) for whole-body and serum. Serum data was also used to determine pharmacokinetic parameters, including concentration at 0 time (C_0), $T_{1/2\beta}$, volume of distribution of central compartment, area under the curve (AUC), and systemic clearance. The total %IA initially present in the serum was

estimated by multiplying the %IA/L in serum at C_0 by the patient's estimated plasma volume determined from a nomogram (*23*).

Normal-tissue Dosimetry

Image-derived SUV_{LBM} were converted to activity concentration per unit mass (kBq/g). The AUC were estimated by trapezoidal integration with the contribution of the terminal portion calculated by extrapolation from the last measured value using the faster of apparent terminal clearance rate or physical decay. Subsequently, whole-organ AUCs were estimated by multiplying the activity concentration AUC by organ mass and residence time derived by dividing the AUC by injected activity. Values of standard male/female organ masses were taken from the OLINDA/EXM software (*24*). If the actual body mass was more than 15% greater than the standard value, organ masses were rescaled. The assigned patient mass was the minimum of actual patient mass or a calculated maximum effective mass as previously described (*25*).

The residence time for cardiac contents was calculated by multiplying the serum value (in h/L) by the standard or patient mass-rescaled value of heart contents volume and by (1-measured hematocrit). The residence time for red marrow was calculated as described by Sgouros et al (*26*). The residence time for the remainder of the body was derived by subtracting all the individually estimated residence times for normal organs from the whole-body residence time. Absorbed radiation doses to various normal organs were estimated using OLINDA/EXM software.

Statistics

Descriptive statistics include median or mean and standard deviation. Comparison between groups was done using paired t-test. Statistical analysis was performed with SigmaStat 3.5 (Systat Software Inc, Point Richmond, CA).

RESULTS

Patients

Ten consecutive patients with histologically documented EGA were imaged (esophageal n=2, gastroesophageal junction n=7, and gastric n=1). Tumors were HER2-positive based on immunohistochemistry 3+ (n=8) or 2+ with FISH amplification (n=2). Their median age was 62 years (46-80 y); eight were male and two female. Patients were either trastuzumab-naïve (n=3) or off of trastuzumab for a median of 42 days (range 35-156 days) with the exception of patient #5, who received trastuzumab within 15 days prior to ^{89}Zr-trastuzumab.

Adverse Events

Two patients reported Grade 1 chills during injection that resolved after diphenhydramine and acetaminophen. One patient had chills that did not require treatment, possibly related to ^{89}Zr-trastuzumab administration. No other related adverse events were reported.

Pharmacokinetics

The pharmacokinetics parameters for ^{89}Zr-trastuzumab are shown in Table 1. At the end of infusion, the estimated total activity in serum was a median of 102% (range 78-113%) of the injected dose determined by multiplying the patients' estimated plasma volume by the concentration in serum at the initial sampling time point. The serum volume of distribution of central compartment was within a median of 3% (range -10-28%) of the estimated plasma volume. The median biologic $T_{1/2\beta}$ was 111 h (range 78-193 h) (Supp. Fig. 2A).

Biodistribution

Whole-body retention of activity was prolonged with a median biologic half-time of 370 h (range 257-578 h), as shown in Supp. Figure 2B. Excretion in the urine in the first 1.7 h (range 1.1-2.5 h) was minimal, with a median of 1.6% (range -1.0-7.6%). Whole-body excretion over a median of 120 h (range 115-191 h) was a median of 21.3% (range 16.7-30.0%). In 7 out of the 10 patients, the gallbladder was visualized in the day-of-injection image, but seldom in subsequent images. All patients had bowel visualization that moved over time, consistent with intraluminal content. Exactly how much of the total excretion was urinary versus bowel was not determined; however, bowel appeared to be the predominant route of excretion based on visual inspection.

Optimal tumor visualization was generally obtained at the last imaging time point (5-8 days post-injection), when most lesions were observed with the

best contrast based on visual assessment by an expert reader and with the highest or near highest $SUV_{LBM\text{-}max}$ (Fig. 1). The initial image primarily showed blood pool and rarely any tumor lesions. Tumor uptake typically increased over time, with the highest uptake most often seen at the last time point (Fig. 2). The highest tumor $SUV_{LBM\text{-}max}$ observed ranged from no uptake in any lesion in two patients to a median $SUV_{LBM\text{-}max}$ of 6.8 (range 2.9-22.7) for 20 lesions in seven patients with positive scans, imaged between 115 and 191 h post-administration. The time course of normal organ uptake is shown in Figure 3A. The uptake in liver was relatively low and stable over time as was kidney (with the exception of the last time point representing a single patient). The uptake decreased continuously in blood pool, lung, and spleen. A slight increase in organ-to-blood ratio was observed for liver, kidney, and bone marrow (Fig. 3B).

Tumor Imaging

In 80% of imaged patients, accumulation of ^{89}Zr-trastuzumab tracer was noted in sites of known disease. Focal areas of ^{89}Zr-trastuzumab uptake were seen within known metastatic sites in the liver, lymph nodes, lung, and bone, as well as remaining primary. No uptake was seen in two patients on ^{89}Zr-trastuzumab PET. In patient #4, this was likely due to weak HER2 staining (immunohistochemistry 2+/FISH HER2/CEP17 3.4) and focal HER2 expression. In patient #3 with prior gastrectomy, whose primary tumor and biopsy-proven lung metastasis exhibited strong HER2 expression (immunohistochemistry 3+), ^{89}Zr-trastuzumab PET failed to pick up small volume recurrent disease in a 1.1 x

1.1 cm lung nodule and 1.9 x 1.3 cm retroperitoneal lymph node that were visualized on CT. The retroperitoneal lymph nodes were never biopsied or tested for HER2 over-expression. Patient #8 with very low uptake in bone lesions and no uptake in liver and nodal lesions was receiving chemotherapy at the time of imaging. Heterogeneity of tumor uptake within patients is shown in Supplemental Table 1, along with last trastuzumab therapy since this treatment may compete for tumor uptake.

Absorbed Dose to Normal Organs

The dosimetry estimates from OLINDA are shown in Table 2, indicating that the organs receiving the highest absorbed doses were liver, heart wall, kidney, lung, and spleen with mean values of 1.32, 1.12, 0.9, 0.81, and 0.8 mGy/MBq, respectively. The mean effective dose was 0.48 mSv/MBq.

DISCUSSION

Our data demonstrates for the first time that ^{89}Zr-trastuzumab PET is specific for HER2-positive EGA and visualizes primary tumors and metastases with high contrast. Similar findings have been described previously in patients with breast cancer (*7-10,18*). ^{89}Zr-trastuzumab PET has a potential advantage over single-site biopsies, as it can non-invasively assess variation in level of HER2 and target engagement in both the primary tumor and all sites of metastases simultaneously. ^{89}Zr trastuzumab PET has already been used as a

biomarker in the theranostic setting for breast cancer patients treated with trastuzumab emtansine antibody drug conjugate. In that setting, combining ^{89}Zr-trastuzumab and FDG PET predicted response to treatment with trastuzumab emtansine (*10*). In addition, early changes in ^{89}Zr-trastuzumab uptake in breast cancer metastasis following treatment with heat shock protein 90 inhibitor have correlated with CT changes in the size of lesions (*9*). Lastly, a preliminary report has suggested that breast cancer patients with prior HER2-negative biopsies may be identified as HER2-positive on imaging and selected for therapeutic intervention that they would not otherwise receive (*8*).

In this study, the biodistribution and imaging of ^{89}Zr-trastuzumab in patients with EGA appeared visually similar to that in patients with metastatic breast cancer (*7,8,18*). Recent analysis of ^{89}Zr-trastuzumab biodistribution in normal organs of females with breast cancer has been expressed as %ID (*18*), when our data in SUV_{LBM} is converted to %ID using “standard man” body weight and organ volumes; we obtained uptake values in the same range (data not shown). A prior study with ^{89}Zr-cmAb-U36 antibody in head and neck cancer (*12*) showed similar biodistribution and %ID in liver, spleen, and kidney as previously described in breast cancer patients (*18*). In contrast, some antibodies have higher concentration in organs such as liver (*15,17,27*) or spleen (*16*), which is probably due to cross-reactivity with antigen in these organs and/or the mass amount of antibody used. In our study, the uptake in liver, kidney, and bone marrow showed little increase over time (Fig. 3A). When the ratios of these organs to blood pool was determined, there was evidence of slight accumulation

of ^{89}Zr above blood pool in liver, kidney, and bone marrow (Fig. 3B), whereas the ratios in lung and spleen were flat, suggesting no concentration above blood pool (Fig. 3B).

Our dosimetric findings predominantly in males are in line with those described for ^{89}Zr-trastuzumab in females, where the maximal absorbed dose was to liver, kidney, spleen, and lung (*18*). Interestingly, for the few other ^{89}Zr-labeled antibodies, the dosimetry in most normal organs is in the same range as for ^{89}Zr-trastuzumab. The effective dose in our study of 0.48 mGy/MBq was comparable to 0.53, 0.36, 0.41, 0.61, and 0.41 mGy/MBq for cmAB-U36, hJ591, IAB2M minibody, cetuximab, and rituximab antibodies, respectively (*12,15-17,27*). The major difference in organ dosimetry for these ^{89}Zr-labeled antibodies is in the liver and spleen when antibodies cross-reacted with these tissues (*15,16*). It is possible that changing the mass of antibody administered, or if recent trastuzumab were administered, this could result in not only differences in tumor targeting but in biodistribution and dosimetry. This effect of antibody mass in organ dosimetry has been demonstrated with rituximab, where a pre-injection of cold antibody will significantly decrease the dose to the spleen by blocking uptake (0.73 vs. 4.1 mSv/MBq).

We have previously reported that while localization can be achieved with shorter-lived positron-labeled Ga-68 or Cu-64-trastuzumab, their targeting is suboptimal (*28,29*), given the biologic half-life of intact antibody in the circulation for ^{89}Zr-trastuzumab in this study (111 h). In our study, we conclude that the 5-8-day point offered the best imaging, similar to previous studies (*7,18*). Similar

conclusions regarding optimal delayed imaging time with other ^{89}Zr-labeled intact antibodies have been reported (*12,17*). Although studies have shown targeting of ^{111}In-labeled trastuzumab (*30*), the advantage of ^{89}Zr-trastuzumab is its ability to perform quantitative imaging with PET and the higher sensitivity and resolution of PET compared to single-photon emission tomography with ^{111}In.

In this study, we administered ~185 MBq, resulting in good images even at 5-8 days post-administration. Others have used ~37 MBq successfully, although they have pointed out limitations in imaging and defining volume of interest for delayed scans, especially in large patients and delayed times (*7,12,14*). Studies with ^{89}Zr-trastuzumab using 62 MBq showed that delayed imaging could be adequately performed. Based on visual data from our images and prior reports, we believe that we will be able to decrease the administered activity significantly from 185 MBq and still obtain adequate images in patients with EGA (*7,18*).

Adverse events from ^{89}Zr-trastuzumab administration were minor and similar to that observed previously with other ^{89}Zr-labeled antibodies, for which Grade 1 infusion reactions have been observed (*9,12,17,27*).

CONCLUSION

In conclusion, the current study demonstrates the feasibility of using ^{89}Zr-trastuzumab to localize HER2-positive gastric cancer, raising the potential of using this reagent to select or identify patients with gastric cancer who are likely to respond to HER2-directed treatment. Additional patient accrual is ongoing to

further categorize the heterogeneity of uptake and correlate imaging findings with response to HER2-directed therapies.

DISCLOSURE

Mr. William H. and Mrs. Alice Goodwin and the Commonwealth Foundation for Cancer Research, The Center for Experimental Therapeutics of MSK, the Radiochemistry & Molecular Imaging Probes Core (NIH/NCI Cancer Center Support Grant P30 CA008748), the Ludwig Center for Cancer Immunotherapy at MSK, the Conquer Cancer Foundation (Career Development Award, to YYJ), the Department of Defense Congressionally Directed Medical Research Program (CA 150646, to YYJ, JSL, WAW), and the Geoffrey Beene Cancer Research Center at MSK (to JSL). YYJ has received funding, or has pending grants or patents, from Boehringer Ingelheim, Bayer, Genentech, Bristol-Myers Squibb, Eli Lilly, Pfizer, and Merck.

ACKNOWLEDGMENTS

We thank Jing Qiao, Ariel Brown, and staff of the MSK Radiochemistry and Molecular Imaging Probe Core for labeling and dispensing the antibody. We also thank Rashid Ghani of the Nuclear Medicine Pharmacy, the Nuclear Medicine nurses Amabelle Lindo and Louise Harris for their help in patient management, RSA Abigail Boswell and CRM Bolorsukh Gansukh for their excellent support with patient flow and protocol management, the nuclear medicine technologists for their excellent technical assistance, and members of the Department of

Medicine at MSK for patient referral. We thank Leah Bassity for her helpful suggestions in editing this manuscript and its submission to the journal.

REFERENCES

1. Siegel RL, Miller KD, Jemal A. Cancer statistics, 2016. *CA Cancer J Clin.* 2016;66:7–30.
2. Janjigian YY, Werner D, Pauligk C, et al. Prognosis of metastatic gastric and gastroesophageal junction cancer by HER2 status: a European and USA International collaborative analysis. *Ann Oncol.* 2012;23:2656–62.
3. Bang YJ, Van Cutsem E, Feyereislova A, et al. Trastuzumab in combination with chemotherapy versus chemotherapy alone for treatment of HER2-positive advanced gastric or gastro-oesophageal junction cancer (ToGA): a phase 3, open-label, randomised controlled trial. *Lancet.* 2010;376:687–697.
4. Ock CY, Lee KW, Kim JW, et al. Optimal patient selection for trastuzumab treatment in HER2-positive advanced gastric cancer. *Clin Cancer Res*. 2015;21:2520–2529.
5. Gajria D, Chandarlapaty S. HER2-amplified breast cancer: mechanisms of trastuzumab resistance and novel targeted therapies. *Expert Rev Anticancer Ther.* 2011;11:263–275.
6. Janjigian YY, Viola-Villegas N, Holland JP, et al. Monitoring afatinib treatment in HER2-positive gastric cancer with ^{18}F-FDG and ^{89}Zr-trastuzumab PET. *J Nucl Med.* 2013;54:936–943.
7. Dijkers EC, Munnink THO, Kosterink JG, et al. Biodistribution of Zr-89-trastuzumab and PET imaging of HER2-positive lesions in patients with metastatic breast cancer. *Clin Pharmacol Ther.* 2010;87:586–592.

8. Ulaner GA, Hyman DM, Ross DS, et al. Detection of HER2-positive metastases in patients with HER2-negative primary breast cancer using ^{89}Zr-trastuzumab PET/CT. *J Nucl Med.* 2016;57:1523–1528.
9. Gaykema SBM, Schroder CP, Vitfell-Rasmussen J, et al. Zr-89-trastuzumab and Zr-89-bevacizumab PET to evaluate the effect of the HSP90 inhibitor NVP-AUY922 in metastatic breast cancer patients. *Clin Cancer Res.* 2014;20:3945–3954.
10. Gebhart G, Lamberts LE, Wimana Z, et al. Molecular imaging as a tool to investigate heterogeneity of advanced HER2-positive breast cancer and to predict patient outcome under trastuzumab emtansine (T-DM1): the ZEPHIR trial. *Ann Oncol.* 2016;27:619–624.
11. Bahce I, Huisman MC, Verwer EE, et al. Pilot study of Zr-89-bevacizumab positron emission tomography in patients with advanced non-small cell lung cancer. *EJNMMI Res.* 2014;4:35.
12. Borjesson PKE, Jauw YWS, de Bree R, et al. Radiation dosimetry of Zr-89-labeled chimeric monoclonal antibody U36 as used for immuno-PET in head and neck cancer patients. *J Nucl Med.* 2009;50:1828–1836.
13. Gaykema SBM, Brouwers AH, Lub-de Hooge MN, et al. Zr-89-bevacizumab PET imaging in primary breast cancer. *J Nucl Med.* 2013;54:1014–1018.
14. Lamberts LE, van Oordt C, ter Weele EJ, et al. ImmunoPET with anti-mesothelin antibody in patients with pancreatic and ovarian cancer before

anti-mesothelin antibody-drug conjugate treatment. *Clin Cancer Res.* 2016;22:1642–1652.

15. Makris NE, Boellaard R, van Lingen A, et al. PET/CT-derived whole-body and bone marrow dosimetry of Zr-89-cetuximab. *J Nucl Med.* 2015;56:249–254.

16. Muylle K, Flamen P, Vugts D, et al. Tumour targeting and radiation dose of radioimmunotherapy with Y-90-rituximab in CD20+B-cell lymphoma as predicted by Zr-89-rituximab immuno-PET: impact of preloading with unlabelled rituximab. *Eur J Nucl Med Mol Imaging.* 2015;42:1304–1314.

17. Pandit-Taskar N, O'Donoghue JA, Beylergil V, et al. Zr-89-huJ591 immuno-PET imaging in patients with advanced metastatic prostate cancer. *Eur J Nucl Med Mol Imaging.* 2014;41:2093–2105.

18. Laforest R, Lapi SE, Oyama R, et al. [^{89}Zr]Trastuzumab: evaluation of radiation dosimetry, safety, and optimal imaging parameters in women with HER2-positive breast cancer. *Mol Imaging Biol*. 2016;18:952–959.

19. Vosjan M, Perk LR, Visser GWM, et al. Conjugation and radiolabeling of monoclonal antibodies with zirconium-89 for PET imaging using the bifunctional chelate p-isothiocyanatobenzyl-desferrioxamine. *Nat Protoc.* 2010;5:739–743.

20. Holland JP, Sheh YC, Lewis JS. Standardized methods for the production of high specific-activity zirconium-89. *Nucl Med Biol.* 2009;36:729–739.

21. Lindmo T, Boven E, Cuttitta F, Fedorko J, Bunn PA. Determination of the immunoreactive fraction of radiolabeled monoclonal-antibodies by linear

extrapolation to binding at infinite antigen excess. *J Immunol Methods.* 1984;72:77–89.

22. Barrett PHR, Bell BM, Cobelli C, et al. SAAM II: Stimulation, analysis, and modeling software for tracer and pharmacokinetic studies. *Metabolism.* 1998;47:484–492.

23. Retzlaff JA, Tauxe WN, Kiely JM, Stroebel CF. Erythrocyte volume, plasma volume, and lean body mass in adult men and women. *Blood.* 1969;33:649–661.

24. Stabin MG, Sparks RB, Crowe E. OLINDA/EXM: The second-generation personal computer software for internal dose assessment in nuclear medicine. *J Nucl Med.* 2005;46:1023–1027.

25. Wahl RL, Kroll S, Zasadny KR. Patient-specific whole-body dosimetry: principles and a simplified method for clinical implementation. *J Nucl Med.* 1998;39:14S–20S.

26. Sgouros G, Stabin M, Erdi Y, et al. Red marrow dosimetry for radiolabeled antibodies that bind to marrow, bone, or blood components. *Med Phys.* 2000;27:2150–2164.

27. Pandit-Taskar N, O'Donoghue JA, Ruan ST, et al. First-in-human imaging with Zr-89-Df-IAB2M anti-PSMA minibody in patients with metastatic prostate cancer: pharmacokinetics, biodistribution, dosimetry, and lesion uptake. *J Nucl Med.* 2016;57:1858–1864.

28. Carrasquillo JA, Morris PG, Humm JL, et al. Copper-64 trastuzumab PET imaging: a reproducibility study. *Q J Nucl Med Mol Imaging*. 2016 May 12 [Epub ahead of print].

29. Beylergil V, Morris PG, Smith-Jones PM, et al. Pilot study of ^{68}Ga-DOTA-F(ab')2-trastuzumab in patients with breast cancer. *Nucl Med Commun*. 2013;34:1157–1165.

30. Perik PJ, Lub-De Hooge MN, Gietema JA, et al. Indium-111-labeled trastuzumab scintigraphy in patients with human epidermal growth factor receptor 2-positive metastatic breast cancer*. J Clin Oncol*. 2006;24:2276–2282.

FIGURES

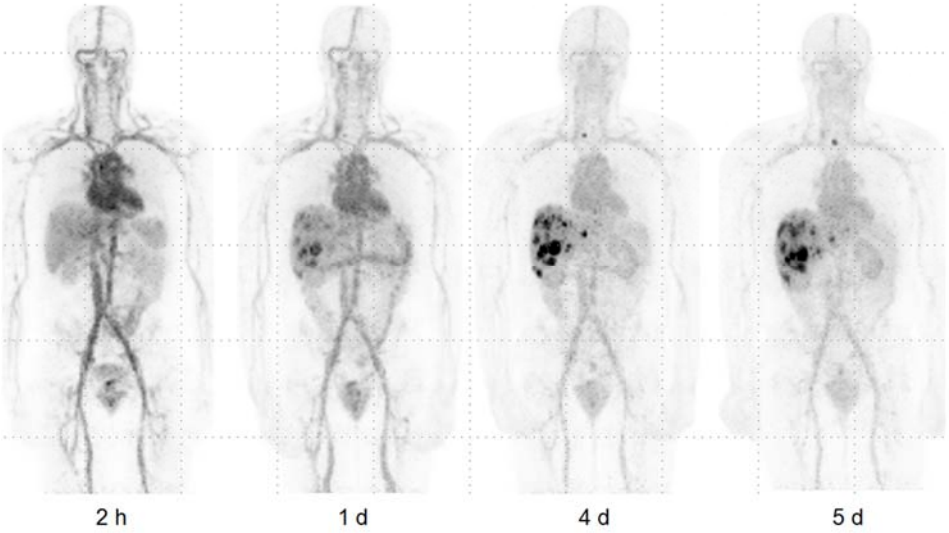

FIGURE 1. Patient #10 with EGA cancer metastatic to the liver. Serial MIP images are shown, following injection of 182.8 MBq of ^{89}Zr-trastuzumab. All images are of good quality up to 5 days post-injection (images set to same gray scale). Immediate post-injection images do not show tumor uptake. Images at one day post-injection show uptake in metastatic liver lesions that increases over time and are well identified at 4 and 5 days post-injection with $SUV_{LBM\text{-}max}$ of 22.7. Foci in upper mediastinal nodes is best seen at 5 days post-injection. Blood pool activity decreases over time. Activity in bowel is present at all time points. Minimal/no activity seen in urinary bladder.

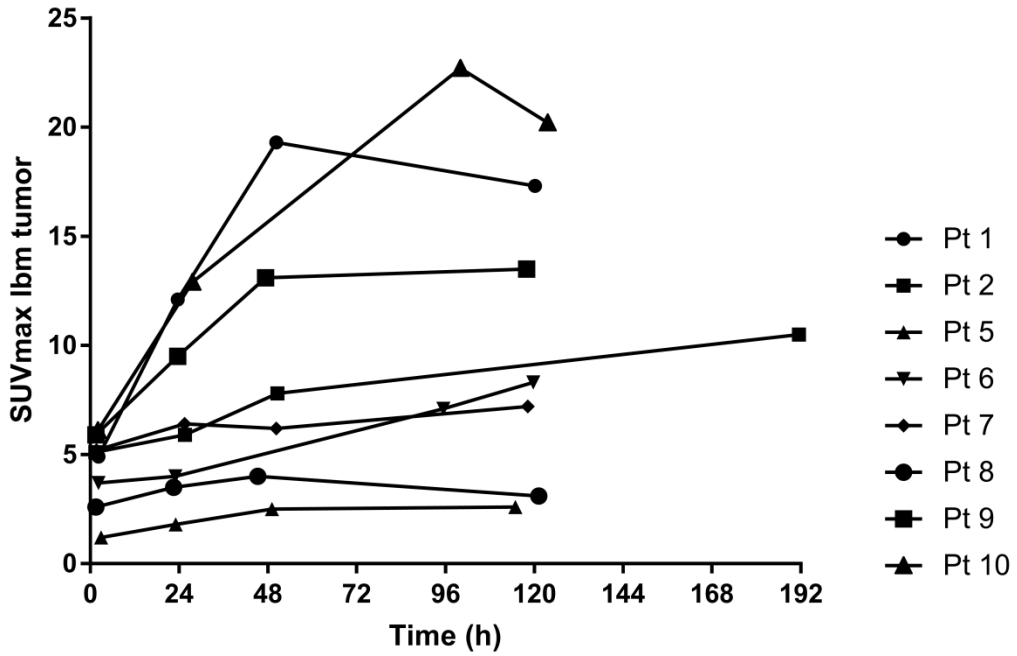

FIGURE 2. Volume of interest drawn over tumor lesions with highest uptake ($SUV_{LBM\text{-}max}$ (8 patients) with ^{89}Zr-trastuzumab uptake usually increasing over time with highest $SUV_{LBM\text{-}max}$ typically at >48 h) post-injection.

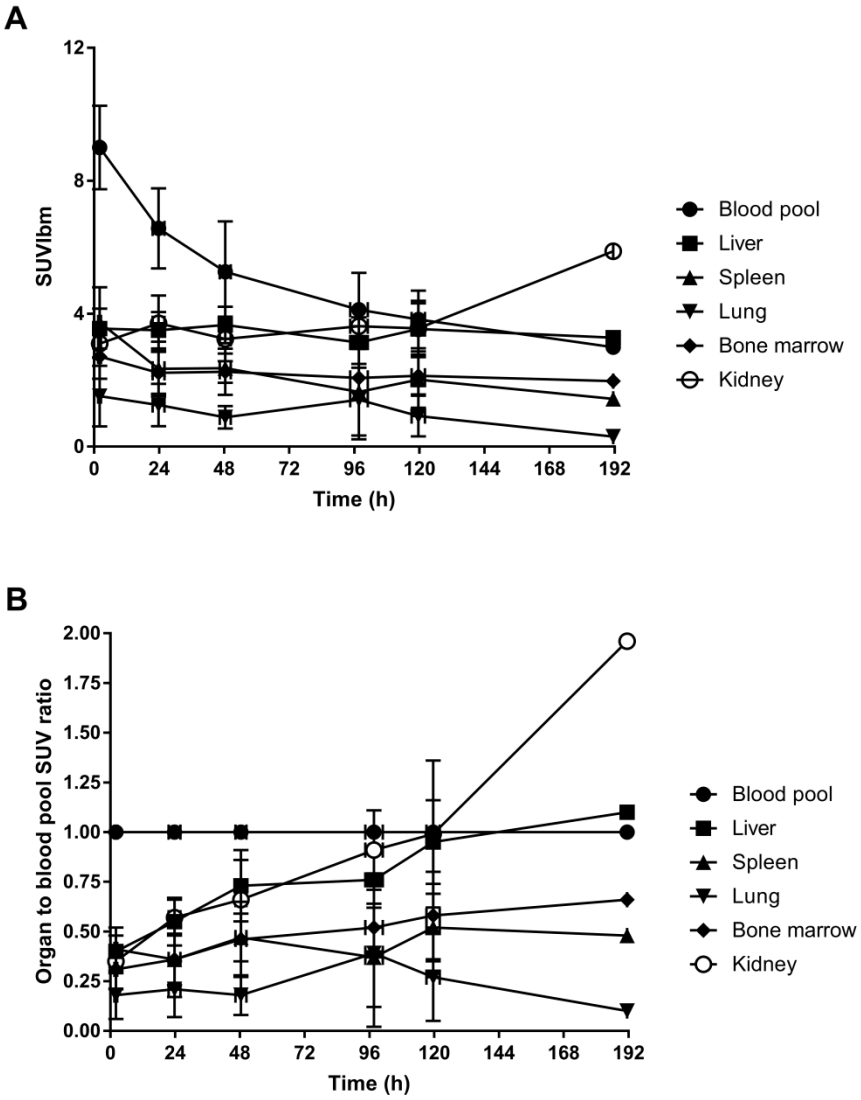

FIGURE 3. (A) SUV_{LBM} was determined by placing volume of interest over various organs and was averaged over all available time points (n=10 for 2 h and 24 h, n=9 for 48 h, n=2 for 96 h, n=10 for 120 h, and n=1 for 192 h). SUVs were fairly stable over time for bone marrow, liver, as well as kidney, except for the last

time point. A slight decrease in SUV_{LBM} was noted for spleen and lung, as was a larger decrease in activity in blood. (B) Organ-to-blood-pool ratios show fairly stable changes for spleen and lung over time, suggesting no concentration above blood pool. In contrast, liver, kidney, and bone marrow showed a slight increase over time, suggesting some ^{89}Zr accumulation in these organs.

TABLE 1. Pharmacokinetic parameters for ^{89}Zr-trastuzumab

Parameter	Median	Min	Max
Co-measured (% injected activity/ liter)	31.56	24.5	46.7
Co-fit (% injected activity/ liter)	31.55	24.4	44.8
Vd (L)	3.17	2.23	4.10
$T_{1/2\alpha}$ (h)	3.1	1.9	15.3
$T_{1/2\beta}$ (h)	111	78	193
Clearance (mL/h)	28.8	12.2	52.5
Estimated amount in plasma volume (%)	102	78	113

TABLE 2. Normal organ-absorbed doses for ^{89}Zr-trastuzumab. Units are mGy/MBq unless otherwise noted.

Target organ	Mean	SD	Median	Min	Max
Adrenals	0.57	0.08	0.57	0.47	0.73
Brain	0.24	0.05	0.25	0.16	0.31
Breasts	0.31	0.05	0.31	0.23	0.38
Gallbladder wall	0.64	0.08	0.65	0.52	0.78
LLI wall	0.43	0.10	0.42	0.32	0.65
Small intestine	0.40	0.06	0.42	0.30	0.47
Stomach wall	0.43	0.07	0.44	0.32	0.54
ULI wall	0.44	0.07	0.44	0.35	0.55
Heart wall	1.12	0.18	1.12	0.85	1.46
Kidneys	0.90	0.22	0.78	0.68	1.26
Liver	1.32	0.24	1.37	0.90	1.75
Lungs	0.81	0.18	0.77	0.58	1.17
Muscle	0.33	0.05	0.33	0.23	0.40
Ovaries	0.38	0.07	0.40	0.26	0.47
Pancreas	0.56	0.09	0.56	0.45	0.71
Red marrow	0.45	0.08	0.45	0.32	0.61
Osteogenic cells	0.50	0.11	0.50	0.32	0.69
Skin	0.23	0.04	0.23	0.16	0.29
Spleen	0.80	0.19	0.74	0.59	1.20
Testes	0.26	0.05	0.27	0.17	0.30
Thymus	0.46	0.06	0.47	0.34	0.55
Thyroid	0.31	0.05	0.32	0.21	0.36
Urinary bladder wall	0.33	0.05	0.34	0.23	0.38
Uterus	0.38	0.07	0.39	0.25	0.46
Total body	0.37	0.06	0.37	0.28	0.46
Effective dose equivalent (mSv/MBq)	0.60	0.09	0.60	0.49	0.76
Effective dose (mSv/MBq)	0.48	0.06	0.47	0.38	0.57

SUPPLEMENTARY DATA

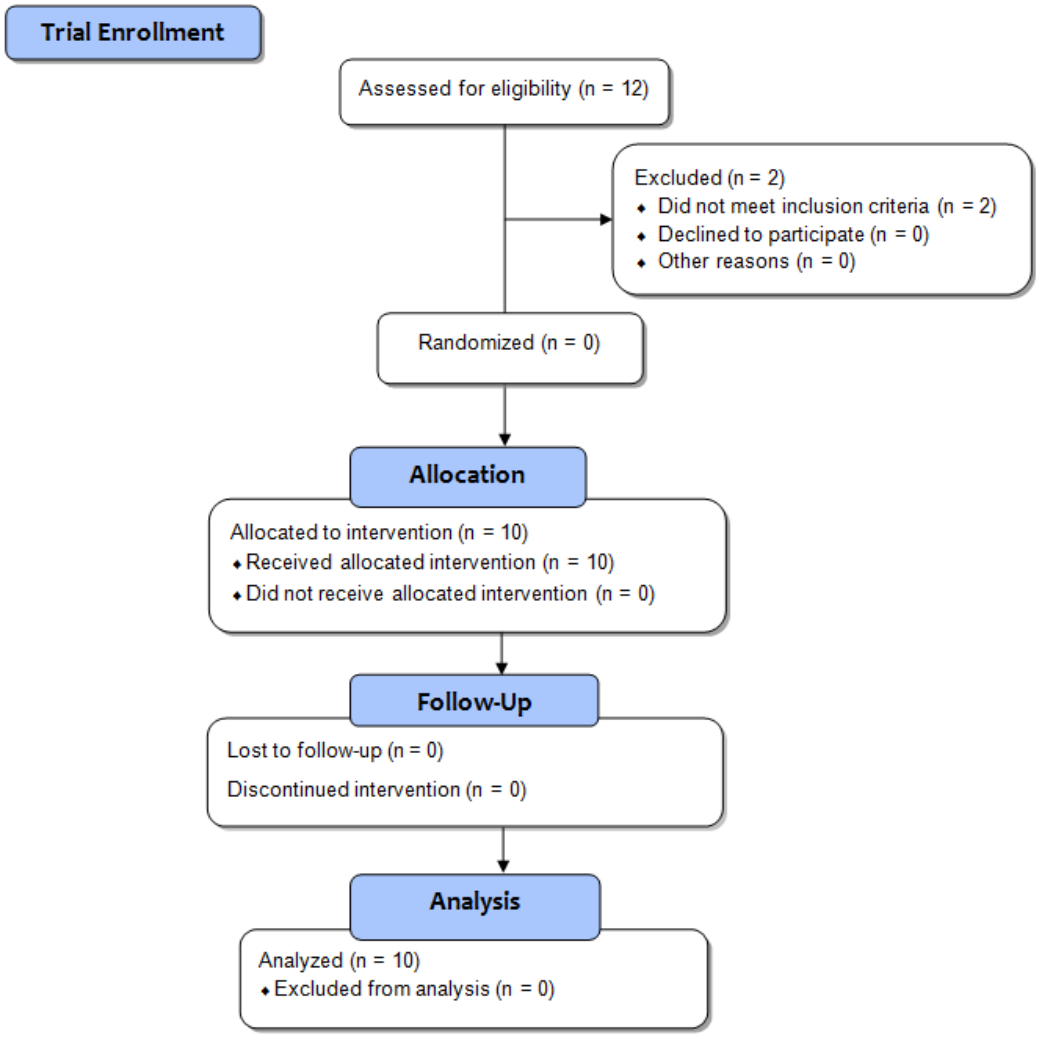

SUPPLEMENTARY FIGURE 1. CONSORT diagram for *Pilot Trial of PET Imaging with ^{89}Zr-DFO-Trastuzumab in Esophagogastric Cancer*. All patients in cohort 1.

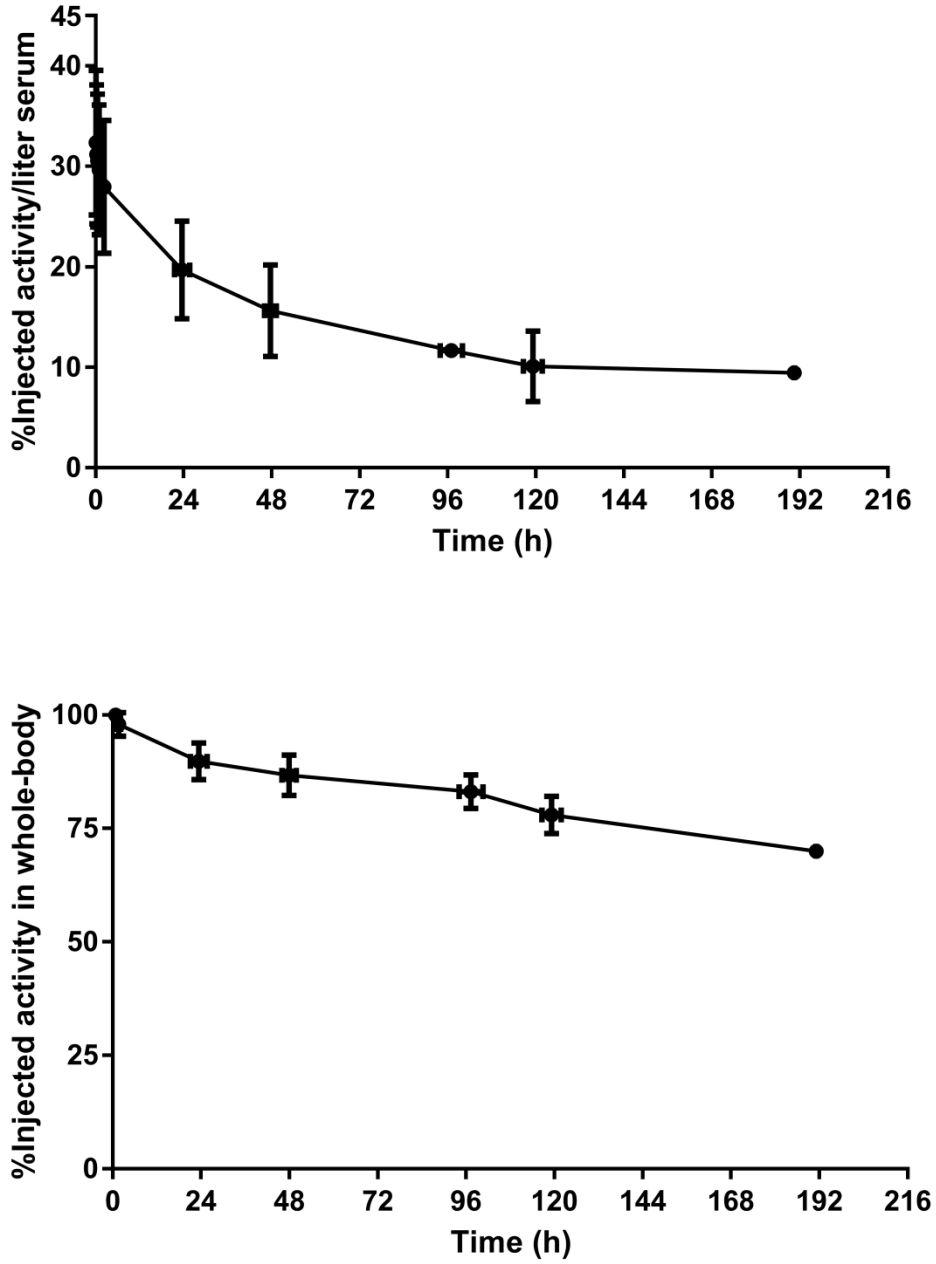

SUPPLEMENTARY FIGURE 2. The concentration of ^{89}Zr-trastuzumab in serum was determined by counting serum samples in a gamma well counter from 10 patients (upper panel). The average serum concentration (%IA/L) ± SD was

plotted against time (h) ± SD. Initially, most of the entire injected activity was present in the serum, which cleared with a median T1/2 of 111 h. Whole-body clearance of activity was determined by using serial probe measurement (lower panel). The initial probe measurement was done after injection of ^{89}Zr-trastuzumab and prior to voiding, and thus represented 100% of the injected activity. Whole-body retention was prolonged with a median T1/2 378 h. At a mean of 120 h, there was a mean retention of 70-83% of the injected activity in the whole body.

Patient	Tumor 1	Tumor 2	Tumor 3	Tumor 4	Tumor 5	Time of last trastuzumab therapy prior to ^{89}Zr-trastuzumab (days)
1	19.3	12.8	7.3	5.4		-71
2	10.5	8.3	8.1	6.4	6.1	-42
3	Negative					Naïve
4	Negative					-35
5	3.2	3.0	2.9	2.2	2.2	-15
6	8.3	7.5	7.0	6.2	3.9	-106
7	7.2	5.8	4.0			-41
8	3.1	2.9				Naïve
9	13.5	12.6	12.5	10.9	8.4	Naïve
10	22.7	11.6	10.8	9.8	9.2	-156

SUPPLEMENTARY TABLE 1. Highest ^{89}Zr-trastuzumab SUV_{LBMmax} uptake in up to 5 lesions identified per patient and demonstrated heterogeneity in the degree of tumor uptake. Patients 3 and 4 had no localization in any of their known tumor sites. The last column indicates the number of days from the last cold trastuzumab therapy to injection of ^{89}Zr-trastuzumab.